Motion of a two-dimensional monopolar vortex in a bounded rectangular domain

J. H. G. M. van Geffen,[a] V. V. Meleshko,[b] and G. J. F. van Heijst
Fluid Dynamics Laboratory, Department of Applied Physics, Eindhoven University of Technology, P.O. Box 513, 5600 MB Eindhoven, The Netherlands

(Received 30 March 1995; accepted 7 May 1996)

In this paper we describe results of a study of the two-dimensional motion of a distributed monopolar vortex in a viscous incompressible fluid in a bounded rectangular domain with free-slip and no-slip boundary conditions. In the case of free-slip walls the motion of the vortex center can be satisfactorily modelled by a single point vortex in an inviscid fluid. Comparison of the results of both models reveals a good quantitative agreement for the trajectories of the vortex centers and of the period of one revolution around the center of the domain, for moderate viscous effects ($\mathrm{Re}=1000$ and more). In a domain with no-slip walls the distributed monopolar vortex moves to the center of the domain along a curved but not smooth trajectory due to the interaction of the monopole and the wall-induced vorticity. © *1996 American Institute of Physics.* [S1070-6631(96)01009-4]

I. INTRODUCTION

Two-dimensional (2D) vortex motion in bounded domains has been studied for quite a long time (Villat[1]; Müller[2]; see also Saffman[3]). Traditionally, the attention was concentrated on the motion of point vortices in an inviscid fluid with so-called ''free-slip'' walls: the normal component of the velocity is equal to zero at the wall, with no restriction on the tangential velocity. An elegant mathematical technique based on Green's function (Saffman[3]) permits us to write a set of ordinary differential equations for the motion of point vortices inside any domain. These equations express in a rather general and concise manner a very extensive class of phenomena. One important conclusion is that a single point vortex, although immovable in an unbounded fluid at rest at infinity, placed in a bounded domain will move due to the velocity field induced by the system of its image vortices.

On the other hand, comparatively little has been done to clarify the influence of viscous effects on the motion of initially compact vorticity distributions in a bounded domain. In this paper we provide a comparative analysis of the motion of a point vortex and of a circular vortex with a non-singular initially axisymmetric vorticity distribution (henceforth referred to as ''monopole'') in an inviscid and viscous fluid, respectively, confined in a rectangular domain with free-slip walls. Such a rather simple and basic configuration offers a better understanding of the possibilities of both models.

In physical reality, however, free-slip walls are not present since there is always friction at the walls. Hence, one would want to apply a ''no-slip'' boundary condition: at the wall the velocity of the fluid equals zero. This condition implies generation of oppositely-signed vorticity near the wall, leading to a flow evolution different from the case of free-slip walls (see, e.g., Orlandi[4]; Verzicco *et al.*[5]). A no-slip boundary condition cannot be applied to point vortices, but it can be applied in the method used for the computations with the distributed monopole, so that the effect of no-slip walls can be studied too.

In the next section the vortex models used in the numerical simulations are discussed. The results of these simulations for free-slip and no-slip domain boundaries are presented in Secs. III and IV, respectively. The paper ends with some general conclusions.

II. MODELS FOR THE VORTEX MOTION IN A RECTANGULAR DOMAIN

The non-stationary 2D flow of an incompressible viscous fluid with distributed vorticity ω is governed by the Navier-Stokes equation, here written in the $(\omega,\psi)-$formulation:

$$\frac{\partial \omega}{\partial t}+J(\omega,\psi)=\nu\nabla^2\omega, \quad \omega=-\nabla^2\psi, \tag{1}$$

where J and ∇^2 are the Jacobian and Laplacian operator, respectively, ψ the streamfunction, and ν the kinematic viscosity. The numerical scheme used to solve the non-linear system (1) is a finite difference method similar to the one used by Orlandi.[4] The main difference with Orlandi[4] is that either free-slip or no-slip boundary conditions are imposed at the walls.

Two initially compact axisymmetric distributions of vorticity in a patch of radius r_0 and centered around $(x_1^{(0)},y_1^{(0)})$ are used, namely

$$\omega(r)=\omega_0, \tag{2a}$$

$$\omega(r)=\omega_0 J_0(kr/r_0), \tag{2b}$$

corresponding to a Rankine vortex and a Bessel-type monopole, respectively, with zero vorticity outside the patch [i.e., $\omega(r>r_0)=0$]. Here $r^2=(x-x_1^{(0)})^2+(y-y_1^{(0)})^2$, and $k=2.4048$ is the first root of the equation $J_0(k)=0$. The third vortex model used is

$$\omega(r)=\omega_0\exp(-r^2/R^2), \tag{2c}$$

[a]Present address: Geophysical and Environmental Fluid Dynamics Laboratory, Department of Civil Engineering, University of Dundee, Nethergate, Dundee, DD1 4HN, United Kingdom.
[b]Also at the Institute of Hydromechanics of the National Academy of Sciences, 252057 Kiev, Ukraine.

usually referred to as a Gaussian monopole (or Lamb vortex; see Saffman and Baker[6]), where R is the length scale of the vortex, which is set equal to $R=r_0$. In all three cases the value of ω_0 is chosen such that the total initial intensity of the vortex is equal to Γ_1. After making (1) dimensionless in the usual way, the Reynolds number Re appears, which can be written as $\mathrm{Re}=\Gamma_1/\nu$.

The motion of a point vortex of constant intensity Γ_1 in an inviscid fluid in a rectangular domain $-a\leqslant x\leqslant a, -b\leqslant y\leqslant b$ bounded by free-slip walls was studied early this century (Villat[1]; Müller[2]); these publications provide the analytical solution of the closed trajectory of the vortex and of the period of a full revolution. The equations of the point vortex motion can, expressed in its coordinates (x_1,y_1), be written in the form of a Hamiltonian system:

$$\frac{dx_1}{dt}=\frac{\partial H_1}{\partial y_1}, \qquad \frac{dy_1}{dt}=-\frac{\partial H_1}{\partial x_1}, \tag{3}$$

with initial conditions $x_1=x_1^{(0)}, y_1=y_1^{(0)}$. Here

$$H_1(x_1,y_1)=-\frac{\Gamma_1}{8\pi}\ln[\wp(2x_1+2a)+\overline{\wp(}2y_1+2b)], \tag{4}$$

where $\wp(z)$ and $\overline{\wp(}z)$ are the Weierstrass rho functions (Abramowitz and Stegun[7]) with half-periods $2a$, $2ib$ and $2b$, $2ia$, respectively.

The trajectory of the vortex in the rectangle is a closed curve defined by

$$H_1(x_1,y_1)=H_1(x_1^{(0)},y_1^{(0)}). \tag{5}$$

For the initial position of the vortex not too close to the walls the trajectory resembles an ellipse drawn around the center of the rectangle. The period of revolution can be calculated explicitly in the form of an ultra-elliptic integral (Villat[1]). The trajectory of the point vortex is independent of the value of Γ_1, but the period of one full revolution is proportional to $1/\Gamma_1$.

To follow the trajectories of the distributed monopoles a single passive tracer is placed at the initial center of the monopole and it is the trajectory of this tracer which is shown in the figures. A tracer is used because the maximum of vorticity can only be determined at grid points, so that the path of the maximum of vorticity is not a smooth line and can thus not easily be compared with the point vortex' trajectory. Since the fluid is considered to be incompressible a radial motion with respect to the monopole's center is not expected and thus the tracer is expected to remain on the maximum of vorticity, at least as long as there is a (clear) maximum. When the tracer moves away from the maximum it starts making circular orbits around the maximum as the monopole moves through the domain. If this happens, it is mentioned in the text.

The numerical simulations reported in the paper are performed in a square domain with $a=b=3$, and the intensity of the vortices at $t=0$ is $\Gamma_1=1$. In the finite difference method the grid used has 128 cells in either direction (i.e., $\Delta x=\Delta y\approx 0.047$) and the initial radius of the distributed monopoles is $r_0=0.5$.

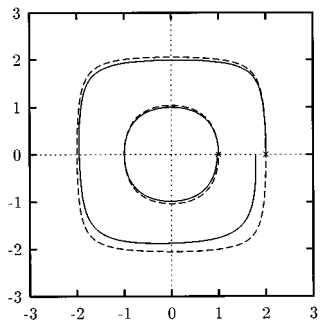

FIG. 1. Trajectories for one full revolution of a Bessel monopole (solid lines) and a point vortex (dashed lines) in a square domain starting either at (1,0) or at (2,0); the initial positions are marked with a cross. For the Bessel monopole the Reynolds number is Re=1000. A Rankine or Gaussian monopole follows the same trajectory as the Bessel monopole. See also Table I.

III. RESULTS FOR A DOMAIN WITH FREE-SLIP WALLS

If a free-slip condition is applied to the walls of the domain, a comparison between the motion of a point vortex and a distributed monopole is possible. Consider first the case of a point vortex and a monopole located initially at (1,0) and with Reynolds number $\mathrm{Re}=\Gamma_1/\nu=1000$.

The results of the simulations, presented in Fig. 1 and Table I, show that the trajectory and the period of one full revolution of both the point vortex and the center of the monopole as well as the moments of crossing the corresponding x and y-axes agree very well for all three types of distributed monopoles. This is especially surprising since in the viscous cases the initially compact vorticity is gradually spread over a larger area and hence the vorticity maximum decreases in time, as shown in Fig. 2. Initially the diameter of the monopoles is 1/6-th of the domain size, but after half a revolution ($t=t_2$; see Fig. 2) the diameter of the monopoles is already larger than 1/3-rd of the domain size and the maximum of vorticity has decreased so much that one can no longer speak of vorticity being concentrated in a small patch. A point vortex would thus seem to be a bad model for the evolved monopoles, yet the motion of the point vortex and the center of the monopoles are in good agreement for one revolution.

The results in Table I show that the orbital period of the initially compact monopolar vortex is only weakly dependent on the initial vorticity distribution. Figure 2 shows that the decay of the three monopoles is quite similar once the first quadrant has been crossed: the vorticity profiles look almost

TABLE I. Times t_1, t_2, t_3, and t_4 at which the center of the vortex initially located at (1,0) successively crosses the coordinate axes for the point vortex and the three distributed monopoles. The Reynolds number is Re=1000. The trajectories of the point vortex and the Bessel monopole are shown in Fig. 1.

Vortex	t_1	t_2	t_3	t_4
Point	95.4	190.7	286.1	381.5
Bessel	93.8	188.4	284.6	383.3
Rankine	93.9	188.9	285.2	384.1
Gaussian	94.0	189.3	286.6	386.8

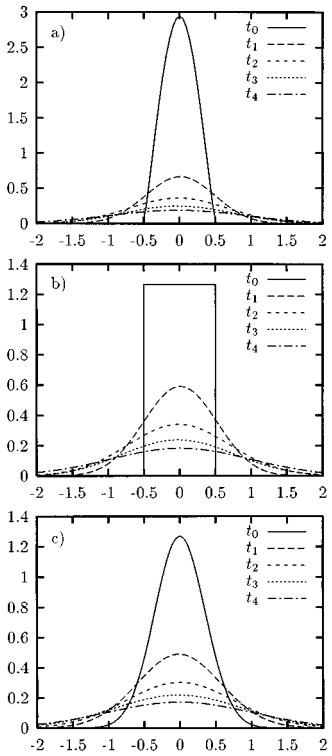

FIG. 2. Profiles of the vorticity distribution along the line through the center of the vortex parallel to the nearest wall at initial time $t=t_0=0$ and at times $t=t_1,t_2,t_3,t_4$ given in Table I. (a) The Bessel-type monopole. (b) The Rankine vortex. (c) The Gaussian monopole. For all three monopoles the Reynolds number is Re=1000.

the same at $t=t_1$ and later on. For the case of the Rankine monopole the decrease of the maximum of vorticity is predicted very well (with a difference of about 0.5%) by the solution of Terazawa[8] and Nekrassow[9] for an infinite domain, which is $\omega_{max}/\omega_0=1-\exp(-r_0^2/4\nu t)$.

As time goes on after one revolution, the vorticity is spread more and more and the maximum of vorticity spirals to the center of the domain. The Bessel monopole, for instance, has completed one revolution at $t=383.3$ when it crosses the x-axis in $x=0.967$, and it has completed a second revolution at $t=826.8$ when it crosses the x-axis in $x=0.761$.

Table II shows the results for a Bessel monopole in the range of Reynolds numbers from 200 to 20,000, and a computation without viscous effects [i.e., (1) with $\nu=0$]. For Reynolds numbers larger than 1000 the period of one revolution decreases somewhat: for large Re the Bessel monopole is about 2% faster than the point vortex. The trajectory of the monopole lies closer to that of the point vortex for higher Reynolds numbers, as expected (not shown): for Re=1000 the center crosses the x-axis after one revolution at $x=0.967$ and for Re=2000 at $x=0.997$. Especially during the first half of a revolution the viscous decay does not affect the motion very much and a point vortex is a good model for the distributed vorticity. For Re=500 the Bessel monopole is only about 1% slower than for Re=1000 at t_2, but after that the vortex decays more and more and at t_4 the difference is about 6%.

TABLE II. Times t_1,t_2,t_3, and t_4 at which the center of the Bessel monopole initially located at (1,0) successively crosses the coordinate axes for different Reynolds numbers Re. The times t_3 and t_4 for Re=200 are not given since then the tracer initially at the center of the monopole is no longer located at the maximum of vorticity; see the text on this. The values for Re=1000 are also given in Table I.

Re	t_1	t_2	t_3	t_4
200	95.3	202.3	—	—
500	94.1	190.7	293.0	404.8
1000	93.8	188.4	284.6	383.3
2000	93.6	187.6	282.0	377.0
5000	93.6	187.3	281.1	375.0
10000	93.6	187.3	281.0	374.6
20000	93.5	187.3	280.9	374.6
∞	93.6	187.0	280.7	374.3

For Re=200 the difference with respect to Re=1000 is at t_2 about 7%. About at that time the tracer initially placed at the maximum of vorticity gradually moves away from the maximum and starts rotating around that maximum as the maximum goes to the center of the domain. Since the maximum of vorticity can only be determined at grid points the moment of time it crosses an axis cannot be found exactly, but only as a range of times when the grid-coordinate of the maximum equals the coordinate of the axis. At $t_3=357\pm4$ the maximum of vorticity crosses the negative y-axis and the positive x-axis is crossed at $t_4=654\pm30$. At $t=1000$ the maximum of vorticity is one grid point away from the center (i.e., about 0.047) and the vorticity is spread over the entire domain almost evenly: the maximum of vorticity is 0.0061 (at $t=0$ it is 2.9448; see Fig. 2).

All in all one can state that for Reynolds numbers larger than 500 the motion of the point vortex is in good agreement with that of the center of the distributed monopole. For lower Reynolds numbers the viscous decay of the vortex is too fast for the vortex to complete one revolution with a clear maximum of vorticity and the point vortex is not an adequate model.

If the initial position of the monopole and the point vortex is shifted nearer to the wall, the quantitative difference in periods becomes more significant, even for Re=1000: for the Bessel monopole and the point vortex, respectively, both initially centered at (2,0) the time for half a revolution is T_{half}(Bessel)=133.3 and T_{half}(PV)=127.8 (a difference of about 4%) and for a full revolution T_{full}(Bessel)=305.1 and T_{full}(PV)=255.6 (about 19% difference). Figure 1 shows the respective trajectories. A Rankine monopole moves along a trajectory quite similar to that of the Bessel monopole, but somewhat slower: T_{half}(Rankine)=135.3 and T_{full}(Rankine)=312.8. The trajectory of a Gaussian monopole lies somewhat inside that of the other two monopoles and it is some 10% slower: T_{half}(Gaussian)=143.2 and T_{full}(Gaussian)=335.7. Clearly the effect of the nearby wall on the distributed vorticity is quite large and depends on the exact initial vorticity distribution.

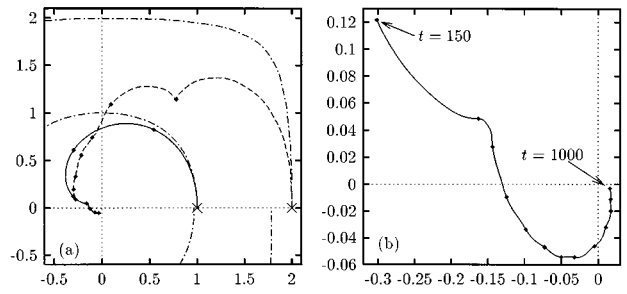

FIG. 3. (a) The path of a Bessel monopole, initially either at (1,0) or at (2,0), in a domain with no-slip walls is shown by a solid and dashed line, respectively, for $t=0$ until $t=500$. Only a part of the full domain is shown for clarity. The symbols are placed at $t=50$, 100, 150, 200, 300, 400, and 500 in both cases. The initial positions are marked with a cross. For comparison, the paths of a Bessel monopole starting at the same positions in a domain with free-slip walls is shown by dash-dotted lines until that monopole has completed one revolution; cf. Fig. 1. (b) Part of the path of a Bessel monopole, initially at (1,0), from $t=150$ until $t=1000$. The symbols are placed at $t=150$, 200, 250, 300, 350, 400, 450, 500, 600, 700, 800, 900, and 1000. [Note that in (b) the vertical scale is not the same as the horizontal.]

IV. RESULTS FOR A DOMAIN WITH NO-SLIP WALLS

A no-slip condition cannot be applied to the walls in the point vortex model since that model cannot handle vorticity generation somewhere in the domain. The effect of no-slip walls on the motion of a distributed monopolar vortex can be studied and compared with its motion in the domain with free-slip walls from the previous section. The computations have been done with all three types of monopoles. If the monopole starts in (1,0) there appears to be little difference in the trajectories the monopoles follow. For (2,0) as a starting point the trajectories are clearly different for the first part of the evolution, but as time goes on and vorticity is spread more and more the evolution of the three monopoles becomes similar again. Because of the difference in evolution the three monopoles are discussed separately, with in all cases the Reynolds number equal to $\mathrm{Re}=1000$.

A. Motion of a Bessel monopole

Figure 3(a) shows a part of the paths of a Bessel monopole starting at initial positions (1,0) and (2,0) for both the no-slip and free-slip boundary conditions. Clearly, the no-slip walls affect the motion of the monopole considerably: it moves away from the wall and tends to drift to the center of the domain along a path that is not a smooth spiral. Continued computation after $t=500$ shows that the monopole indeed approaches the center of the domain closer and closer [Fig. 3(b)]; the closer it gets to the center, the slower is its drift motion. It is not surprising to find that the nearer the monopole initially is to the wall, the larger is the influence of the no-slip walls. In the following, the trajectory of the monopole initially at (1,0) is studied in more detail; the motion of the monopole initially at (2,0) is somewhat more complicated, but not basically different.

Starting at (1,0), the monopole moves along a curved path with slowly decreasing velocity. After $t=200$ the velocity slows down considerably and at about $t=225$ one observes a ''kink'' in the path, as can also be seen in Fig. 3(b).

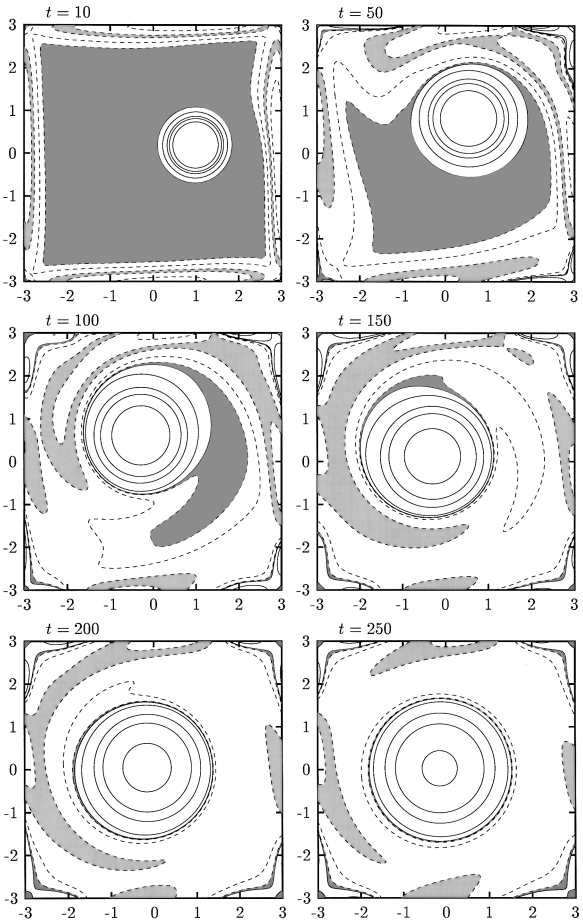

FIG. 4. Contours of vorticity of a Bessel monopole initially at (1,0) at selected moments in time until shortly after the large ''kink'' in the path shown in Fig. 3. Solid lines represent positive vorticity at levels $+0.001$, $+0.01$, $+0.05$, $+0.1$, and $+0.25$. Dashed lines represent negative vorticity at levels -0.001, -0.01, -0.05, -0.1, and -0.25; the latter level is only present in the first three graphs. The areas with vorticity between -0.001 and $+0.001$ (effectively ''zero-vorticity'') and between -0.1 and -0.05 are shaded dark and light, respectively.

Similar kinks, though less pronounced, appear also later on along the path. Performing the same computation at higher grid density (256 cells in either direction, i.e., $\Delta x=\Delta y\approx 0.023$) shows the large kink at the same time at the same location within the domain, indicating that this kink is physical and not just an artifact due to the finite grid size. Some of the smaller kinks in the trajectory after $t=300$ are not: they become less pronounced at higher grid density. At any time of the motion the difference between the trajectories at 128 and 256 grid cells is of the order of 10^{-3}, i.e., much less then the mesh size of the grid.

Figure 4 shows contours of vorticity at selected moments in time until shortly after the large kink in the monopole's path. The areas with vorticity between -0.001 and $+0.001$ (i.e., with effectively ''zero-vorticity'') are shaded to distinguish the monopole's original positive vorticity from the wall-induced negative vorticity. The areas with vorticity between -0.1 and -0.05 (some intermediate level of the induced negative vorticity) are shaded too, but with a somewhat lighter grey.

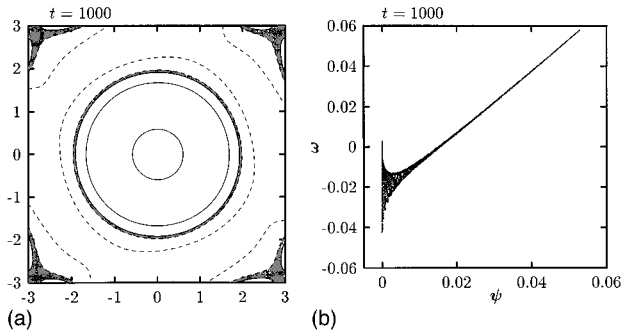

FIG. 5. (a) Contours of vorticity at $t=1000$ of a Bessel monopole initially at (1,0). Solid lines represent positive vorticity at levels $+0.001$, $+0.01$, and $+0.05$. Dashed lines represent negative vorticity at levels -0.001 and -0.01. The areas with vorticity between -0.001 and $+0.001$ (effectively ''zero-vorticity'') are shaded dark. (b) Relationship between vorticity ω and streamfunction ψ of the distribution in (a).

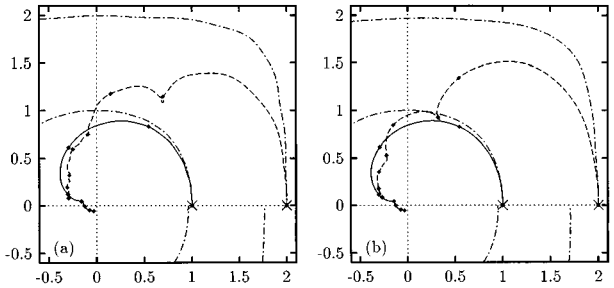

FIG. 6. As Fig. 3(a), but for (a) a Rankine monopole, and (b) a Gaussian monopole.

Initially (not shown in Fig. 4) the whole domain has zero-vorticity, except for the circular region of radius $r_0=0.5$ around (1,0) occupied by the monopole. The no-slip condition at the walls creates negative vorticity, which is then rolled up as the monopole moves (due to the walls) and rotates. At this stage of the evolution the flow field bears some resemblance to a large asymmetric dipolar vortex: the positive monopole is accompanied by an asymmetric negative vorticity distribution which is on one side of the monopole stronger than elsewhere in the domain. Gradually the negative wall-induced vorticity is spread over a larger and larger area due to viscosity, and the asymmetry becomes less and less pronounced. What is left at $t=250$ (bottom-right in Fig. 4) is an almost circular monopolar vortex, located almost at the center of the domain.

The kink in the monopole's path [at about $t=225$; see Fig. 3(b)] occurs when the area of vorticity less then -0.05, forming at $t=200$ a large semi-circular area to the left of the monopole, breaks up in two separate parts left and above the monopole (see $t=250$ in Fig. 4). At about the same moment the asymmetry in the contour of -0.01 (clearly visible at $t=200$) has almost disappeared. The negative induced vorticity is then almost symmetrically distributed around the positive monopole and the asymmetric-dipolar-like behavior becomes less pronounced. Note that from $t=200$ to 250 the motion of (the center of) the vortex is very weak [a travelled distance of about 0.02; Fig. 3(b)] compared with its radius (about 1.5; bottom-right in Fig. 4) at that time.

Continued computation shows that the last asymmetries in the (negative) vorticity gradually disappear after $t=250$. Figure 5(a) shows vorticity contours at $t=1000$: the whole structure is nearly symmetrical with respect to the center of the domain. The tracer initially placed at the center of the monopole remains at the maximum of vorticity throughout its evolution; at $t=1000$ this tracer is at $x=0.016$ and $y=-0.003$. Figure 5(b) shows that the relationship between vorticity ω and streamfunction ψ at $t=1000$ has become linear, except for the contribution of the vorticity in the corners. This linearization in the center of the domain of an initially non-linear ω,ψ-relation is mainly caused by viscous diffusion, as a study of the evolution of a 2D-flow on a square domain by van de Konijnenberg[10] shows.

The straight line $\omega=1.54\psi-0.024$ fits through the straight branch of Fig. 5(b). A Bessel monopole in an infinite fluid, given by (2b), is a (quasi-)stationary axisymmetric solution of the inviscid vorticity equation [i.e., (1) with $\nu=0$]. This solution is based on the assumption of a linear relation between vorticity and streamfunction: $\omega=k^2\psi$, where $ka=2.4048$ with a the radius of the monopole. Assuming that this relation is also valid for the monopolar vortex of Fig. 5, its radius a is $a\approx(2.4048)/\sqrt{1.54}\approx 1.9$, which is in good agreement with Fig. 5(a). Hence, a well-defined branch in the ω,ψ-relation such as in Fig. 5(b) indicates that the flow of the monopolar vortex at the center of the domain has become axisymmetric. The scatter around $\psi=0$ is caused by the advection of vorticity near the walls, where the flow is essentially non-axisymmetric. As time goes on this scatter reduces due to viscous effects.

The trajectory of a Bessel monopole initially at (2,0) shows also some kinks, as can be seen in Fig. 3(a). At $t=51$ there is a rather sharp kink (at $x=0.780$) and between $t=100$ and 150 there is a less pronounced one. The nature of these kinks is the same as of the kink discussed above: the interaction between the positive monopole and the negative wall-induced vorticity. This interaction is evidently more important for a monopole initially located nearer to the wall and it can cause sharp kinks in the monopole's trajectory.

B. Motion of a Rankine monopole

Figure 6(a) shows the trajectories of a Rankine monopole in a domain with no-slip walls, which can be compared with Fig. 3(a). For a monopole starting at (1,0) there is hardly any difference visible between the trajectories of a Bessel and a Rankine monopole (the difference is of the order of the thickness of the lines used in the graphs). A Rankine monopole initially at (2,0) moves along a trajectory similar to that of a Bessel monopole, but not quite the same: the first sharp kink occurs a little later in the evolution (at $t=57.5$) and it is located somewhat more towards the y-axis (at $x=0.694$). It is difficult to see at the scale of Fig. 6(a), but enlarging the graph shows that in fact the center of the monopole performs a small loop there (the tracer used to make the graph it has not moved away from the maximum of

vorticity!). After about $t=80$ the trajectories are almost the same again, though the path of the Rankine monopole is less smooth than the path of the Bessel monopole.

C. Motion of a Gaussian monopole

The motion of a Gaussian monopole in a domain with no-slip boundary conditions also has been computed with a spectral method by Clercx[11] which uses 2D Chebyshev polynomials. A spectral method has the advantage that it resolves the viscous boundary layer near the walls—where rather large vorticity gradients can occur—better than a finite difference method does. The reason for this is that a finite difference method uses an equidistant grid whereas a spectral method uses collocation points which, when Chebyshev polynomials are used, condense near the boundaries. For the monopole initially at (1,0) and (2,0), respectively, 40×40 and 65×65 Chebyshev polynomials are used, meaning that the distance between the first collocation point and the boundaries is about 0.01 and 0.004; the distance between the first and the second collocation point is about 3 times that much. The properties of a spectral method are best used with smooth initial vorticity distributions such as the Gaussian monopole.

A Gaussian monopole initially at (1,0) shows a trajectory—see Fig. 6(b)—which is almost identical to that of a Bessel monopole [Fig. 3(a)]. There is, however, a noticeable difference in the nature of the kink occurring in the trajectory at $t=200-250$: for a Bessel monopole the kink is smooth, whereas for a Gaussian monopole the trajectory shows a rather sharp kink. This is not visible in Fig. 6(b), but the kink is as sharp as that in the trajectory of a monopole starting at (2,0). The location of the kink within the domain and the moment in time when it occurs are the same for the Gaussian and the Bessel monopole. The computations with the spectral method show a trajectory of the Gaussian monopole almost identical to the one it follows with a finite difference method: at any time the difference between the trajectories is of the order of 10^{-3}, and the kink occurs at the same position at the same time and is also sharp. This means that even though the finite difference method resolves the viscous effects near the walls not as good as the spectral method does, the overall effects of the no-slip condition are incorporated quite well by the finite difference method. The correspondence between the results of both methods shows that the kink in the trajectory is of physical origin, as discussed in Sec. IV A.

The reason that the trajectory of the Gaussian monopole shows a sharp kink has presumably something to do with the somewhat larger effect the no-slip condition has: initially the Gaussian monopole has non-zero vorticity near the walls [see Eq. (2c)], whereas the Bessel monopole has zero vorticity outside the initial circle of radius $r_0=0.5$.

Like the other two monopoles, a Gaussian monopole initially at (2,0) moves along a trajectory [see Fig. 6(b)] with a sharp kink, which in fact is a small loop as in the trajectory of the Rankine monopole. But in this case the kink occurs later in the evolution (at about $t=90$) and more towards the y-axis (at $x=0.338$) than the kink of the Bessel and Rankine monopole. A second sharp kink occurs a little later on (at about $t=220$), followed by a motion similar to that of the other two monopoles. At $t=500$ the centers of the three monopoles lie only about 0.02 apart. And due to viscous decay (cf. Fig. 2) the three monopoles will now have almost the same vorticity distribution so that they will continue to move along almost the same trajectory towards the center of the domain.

V. CONCLUSIONS

A distributed two-dimensional monopolar vortex in a bounded domain with free-slip walls moves along the walls of the domain in a manner strikingly similar to the motion of a point vortex of (initially) the same intensity and starting at the same position—in spite of a considerable spreading of the monopole's initial vorticity due to viscosity. This is independent of the precise initial vorticity distribution of the monopole. Thus, the (relatively) simple model of point vortices appears to be rather powerful in describing the main features of the general behavior during one revolution of distributed vortex structures in a bounded domain with free-slip boundaries.

After the first revolution a point vortex continues along the same trajectory. The motion of the distributed monopole depends on viscous effects: viscosity spreads the vorticity over a larger area and thus slows down the monopole, which will thus spiral towards the center of the domain. The higher the Reynolds number is, the longer the monopole remains close to the trajectory of the point vortex. For low Reynolds numbers the viscous decay spreads the vorticity throughout the domain before the monopole has completed one revolution.

In case of a domain with no-slip walls, i.e., zero velocities at the walls, the distributed positive monopole moves along the wall and immediately away from it along a curved but not completely smooth path to the center of the domain as a result of the negative vorticity induced by the walls. The interaction between the positive and negative vorticity causes (sometimes quite sharp) kinks to appear in the trajectory of the monopoles: A large area of positive vorticity—rotating and moving due to the walls—is surrounded by an asymmetric distribution of negative vorticity. This combination acts like a kind of asymmetric dipolar vortex and moves along a curved path, which bends if the negative vorticity area breaks up and is spread around the positive vorticity. The closer the monopole initially is to a boundary, the more negative vorticity is induced near the walls and pulled into the domain and wrapped around the positive monopole as it moves towards the center, and the more important is the precise initial vorticity distribution for the trajectory of the monopole's center.

Due to viscous diffusion, the relationship between vorticity and streamfunction becomes well-defined when the monopole has reached the center of the domain, which implies that the resulting vorticity distribution is axisymmetric.

ACKNOWLEDGMENTS

The authors wish to thank H. J. H. Clercx for many discussions and suggestions and the computations with his

spectral code, which proved to be a useful addition to the paper. This paper was partly written while VVM was visiting the Fluid Dynamics Laboratory in Eindhoven, within the framework of a collaboration project that is financially supported by the Netherlands Organization for Scientific Research (NWO). The research of JHGMvG was financed by the NWO program Non-Linear Systems. The authors gratefully acknowledge these supports.

[1]H. Villat, *Leçons sur la Théorie des Tourbillons* (Gauthier-Villars, Paris, 1930).
[2]W. Müller, ''Bewegung von Wirbeln in einer idealen Flüssigkeit unter dem Einfluss von ebenen Wänden,'' Z. Angew. Math. Mech. **10**, 227 (1930).
[3]P. G. Saffman, *Vortex Dynamics* (Cambridge University Press, Cambridge, 1992).
[4]P. Orlandi, ''Vortex dipole rebound from a wall,'' Phys. Fluids A **2**, 1429 (1990).
[5]R. Verzicco, J.-B. Flór, G. J. F. van Heijst, and P. Orlandi, ''Numerical and experimental study of the interaction between a vortex dipole and a circular cylinder,'' Exp. Fluids **18**, 153 (1995).
[6]P. G. Saffman and G. R. Baker, ''Vortex interactions,'' Annu. Rev. Fluid Mech. **11**, 95 (1979).
[7]M. Abramowitz and I. Stegun, *Handbook of Mathematical Functions* (Dover, New York, 1965).
[8]K. Terazawa, ''On the decay of vortical motion in a viscous fluid,'' Rep. Aeronaut. Res. Inst. Tôkyô Imp. Univ. **1**, N4 (1922).
[9]A. I. Nekrassow, ''On the diffusion of a vortex in a viscous fluid,'' Trans. Central Aero-Hydrodyn. Inst. N. 84, 1 (1931).
[10]J. A. van de Konijnenberg, ''Spin-up in non-axisymmetric containers,'' Ph.D. thesis, Eindhoven University of Technology, The Netherlands, 1995, Appendix A.
[11]H. J. H. Clercx, ''A spectral solver for the Navier–Stokes equations in the velocity–vorticity formulation for flows with non-periodic directions,'' submitted to J. Comput. Phys.